

# Polarization-Angle-Frequency Estimation Using Nested Vector Sensor Arrays

Xiaodong HAN, Ting SHU, Zenghui ZHANG Jin HE, Wenxian YU  
 Shanghai Key Laboratory of Intelligent Sensing and Recognition  
 Department of Electronic Engineering  
 Shanghai Jiaotong University, Shanghai, 200240, P. R. China  
 Email: jinhe@sjtu.edu.cn

**Abstract**—A computationally efficient polarization-angle-frequency estimation algorithm based on spatial-temporal nested sampling is proposed. Radar cross-sections (RCSs) diversity in multiple CPIs is exploited to construct a virtual polarization-spatial-temporal (PST) manifold with extended degree of freedom. A computational efficient method without eigen-decomposition is derived to estimate K-R signal subspace. Automatically paired polarization, azimuth-elevation angles and doppler frequency estimates are obtained by exploiting the idea of the ESPRIT algorithm.

## I. INTRODUCTION

The problem of estimating multiple parameters (including angles, frequencies and polarization) of targets is very important in many application scenarios of radar array processing. Accurate estimation of angle and frequency parameters enables the better target localization and tracking performance, and precise polarization information extraction offers better target classification and recognition performance. During the past decade, many efficient multidimensional parameter estimation methods have been presented. Most of the radar array processing methods consider that the spatio-temporal data samples are taken uniformly with Nyquist rate, and consequently, have limited degree of freedom in both space and time domain. Recently, it is shown that measuring spatial data with nonuniform nested arrays can offer enhanced spatial degree of freedom for angle estimation [1]. Data acquisition with spatially nested sampling has been found in solving various radar signal processing problems such as detection [2], localization [3], [4], and jamming suppression [5].

For multiple dimensional parameter estimation, nested sampling can be exploited in each dimension for use of K-R subspace-based parameter estimation methods with degree of freedom enhancement. For example, [6] develops a two-dimensional angle estimation method using  $L$ -shaped nested array; [7] considers nested sampling in spatial and time delay domains for angle and range estimation; and [8] proposes nested spatio-temporal sampling for joint angle and doppler frequency estimation. The algorithms in [6]-[8] achieve the the degree of freedom enhancement for parameter estimation, however, they have some drawbacks that limit their practical applications. Firstly, the estimation of two-dimensional angles requires the use of planar array geometries, which is unsuitable for some practical situations such as airborne application, where the physical space available for antenna deployment is very limited. Secondly, nested sampling enhances the degree of freedom, but also increases the computational costs involved in

K-R subspace computation, and consequently, these methods are unsuitable for applications where the parameters of targets should be estimated promptly.

Therefore, the purpose of this paper is to investigate the multiple dimensional parameter estimation of radar signals in a geometrically and computationally simple manner. Motivated by the fact that linear vector antenna array can be used to estimate two-dimensional angles [9], we propose a polarization-angle-frequency estimation algorithm using a linear nested vector sensor array. Firstly, radar cross-sections (RCSs) diversity in multiple CPIs to is exploited to construct a virtual polarization-spatial-temporal (PST) manifold with extended degree of freedom. Then, a computational efficient method without eigen-decomposition is derived to estimate K-R signal subspace. Finally, automatically paired polarization, 2D angles and frequency estimates are obtained by using the idea of the ESPRIT algorithm.

*Notation:* Throughout the paper, scalar quantities are denoted by lowercase letters. Lowercase bold type faces are used for vectors and uppercase letters for matrices. Superscripts  $T$ ,  $H$  and  $*$  represent the transpose, conjugate transpose and complex conjugate, respectively,  $\otimes$ ,  $\odot$  and  $\diamond$  symbolize the Kronecker product, Khatri-Rao (column-wise Kronecker) matrix product, and element-by-element multiplication, respectively,  $\mathbf{I}_m$  denotes the  $m \times m$  identity matrix, and  $\mathbf{e}_n$  stands for a vector of all zeros except a 1 at the  $n$ th position.

### A. Transmit Signal Model

For a target located at angle  $(\theta, \phi)$ , the EMVA produces the following  $6 \times 2$  response [10]

$$\mathbf{Q}(\theta, \phi) = \begin{bmatrix} \cos \theta \cos \phi & -\sin \phi \\ \cos \theta \sin \phi & \cos \phi \\ -\sin \theta & 0 \\ -\sin \phi & -\cos \theta \cos \phi \\ \cos \phi & -\cos \theta \sin \phi \\ 0 & \sin \theta \end{bmatrix} \quad (1)$$

where  $\theta \in [0, \pi)$  denotes the elevation angle and  $\phi \in [0, 2\pi)$  represents the azimuth angle. The  $2 \times 1$  baseband unit-power electrical field emitted signal can be expressed as

$$\mathbf{e}(t) = \mathbf{Q}^T(\theta, \phi) \mathbf{w} s(t) = \boldsymbol{\zeta} s(t) \quad (2)$$

where  $\mathbf{w}$  is a  $6 \times 1$  weights that controls the polarization of the transmit signal and  $s(t)$  is the waveform of the transmit signal,  $\boldsymbol{\zeta} = [\zeta_H, \zeta_V]^T$ , where  $\zeta_H \neq 0$  and  $\zeta_V \neq 0$ , respectively,

represent the  $H$ - and  $V$ - components of the waveform [11]. Further, the signal transmitted in each CPI is assumed to have temporal nested structure [8], i.e., it consists of a concatenation of  $M$  uniform pulses, where each is composed of  $N_i$  pulses, with pulse interval  $t_i$ , such that  $\sum_{i=1}^M N_i = N$  and  $t_i = \prod_{j=1}^{i-1} (N_j + 1)t_1, i = 2, \dots, M$ .

### B. Receive Signal Model

Consider that there are  $K$  target signals in a desired range-bin, arriving at the above described radar system. The  $6 \times 1$  down-converted and match-filtered receive signal vector for the  $p$ th pulse, measured by the  $\ell$ th EMVA can be represented as

$$\begin{aligned} \mathbf{x}_\ell(p) &= \sum_{k=1}^K \rho_k(p) \mathbf{Q}(\theta_k, \phi_k) \mathbf{S}_k \boldsymbol{\zeta} a_\ell(\theta_k, \phi_k) e^{j2\pi f_k p} + \mathbf{n}_\ell(p) \\ &= \sum_{k=1}^K \rho_k(p) \mathbf{c}_k a_\ell(\theta_k, \phi_k) e^{j2\pi f_k p} + \mathbf{n}_\ell(p) \end{aligned} \quad (3)$$

where  $\rho_k(p)$  is the RCS-related coefficient of the  $k$ th target at the  $p$ th pulse,  $\mathbf{S}_k$  represents the  $2 \times 2$  scattering matrix, describing the polarization transforming property of the  $k$ th target,  $a_\ell(\theta_k, \phi_k) = e^{-j\frac{2\pi f_c}{c} d_\ell \sin \theta_k \cos \phi_k}$  represents the spatial response of the  $\ell$ th EMVA to the target at  $(\theta_k, \phi_k)$ , in which  $d_\ell$  denotes the position of the  $\ell$ th EMVA, and  $f_c$  is the center frequency of the band,  $\mathbf{n}_\ell(t)$  is the additive Gaussian noise vector, which is assumed to be temporally and spatially white, with zero mean and variances  $\sigma_n^2$ .

In (3),  $\mathbf{d}_k = \mathbf{S}_k \boldsymbol{\zeta}$  denotes the  $2 \times 1$  receive polarization vector of the  $k$ th target, and  $\mathbf{c}_k = \mathbf{Q}(\theta_k, \phi_k) \mathbf{d}_k$  is the  $k$ th target's  $6 \times 1$  EMVA response vector, which has the following representation [10]

$$\begin{aligned} \mathbf{c}_k &= \mathbf{Q}(\theta_k, \phi_k) \begin{bmatrix} \sin \gamma_k e^{j\eta_k} \\ \cos \gamma_k \end{bmatrix} \\ &= \begin{bmatrix} \sin \gamma_k \cos \theta_k \cos \phi_k e^{j\eta_k} - \cos \gamma_k \sin \phi_k \\ \sin \gamma_k \cos \theta_k \sin \phi_k e^{j\eta_k} + \cos \gamma_k \cos \phi_k \\ -\sin \gamma_k \sin \theta_k e^{j\eta_k} \\ -\cos \gamma_k \cos \theta_k \cos \phi_k - \sin \gamma_k \sin \phi_k e^{j\eta_k} \\ -\cos \gamma_k \cos \theta_k \sin \phi_k + \sin \gamma_k \cos \phi_k e^{j\eta_k} \\ \cos \gamma_k \sin \theta_k \end{bmatrix} \end{aligned} \quad (4)$$

where  $\gamma_k \in [0, \pi/2)$  and  $\eta_k \in [-\pi, \pi)$ , respectively, refer to the auxiliary polarization angle and the polarization phase difference of the  $k$ th target. Note that the above EMVA response  $\mathbf{c}_k$  can be expressed as  $\mathbf{c}_k = [\mathbf{e}_k^T, \mathbf{h}_k^T]^T$ , where  $\mathbf{e}_k$  and  $\mathbf{h}_k$  are two  $3 \times 1$  vectors, which represent, respectively, the electric field vector and the magnetic field vector.

Then, the entire  $6L \times 1$  receive data vector of the EMVA array can be expressed as

$$\mathbf{x}(p) = \sum_{k=1}^K (\mathbf{c}_k \otimes \mathbf{a}_k) \rho_k(p) e^{j2\pi f_k p} + \mathbf{n}(p)$$

where  $\mathbf{a}_k = \mathbf{a}(\theta_k, \phi_k) = [a_1(\theta_k, \phi_k), \dots, a_L(\theta_k, \phi_k)]^T$ . Furthermore, we assume that the targets are of Swerling I type, so that they are fluctuating scan-by-scan, i.e.,  $\rho_k(p)$  is invariant during a CPI for collection of  $N$  pulses, and fades independently from CPI to CPI. Hence, we can arrange the

collected data in a CPI-by-CPI format, with the data collected in the  $m$ th CPI being expressed as

$$\mathbf{X}(m) = \mathbf{B}\mathbf{P}(m)\mathbf{G}^T + \mathbf{N}(m) = (\mathbf{C} \odot \mathbf{A})\mathbf{P}(m)\mathbf{G}^T + \mathbf{N}(m) \quad (5)$$

where  $\mathbf{X}(m) = [\mathbf{x}(p_{m,1}), \mathbf{x}(p_{m,2}), \dots, \mathbf{x}(p_{m,N})]$  is an  $6L \times N$  data block, with  $\mathbf{x}(p_{m,n}) = [\mathbf{x}_1(p_{m,n}), \mathbf{x}_2(p_{m,n}), \dots, \mathbf{x}_L(p_{m,n})]^T$  being an  $6L \times 1$  data vector sampled at time  $p_n$  of the  $m$ th CPI,  $\mathbf{B} = \mathbf{C} \odot \mathbf{A} = [\mathbf{c}_1 \otimes \mathbf{a}_1, \dots, \mathbf{c}_K \otimes \mathbf{a}_K]$  denotes the  $6L \times K$  polarization-spatial response matrix, with  $\mathbf{C} = [\mathbf{c}_1, \dots, \mathbf{c}_K]$  and  $\mathbf{A} = [\mathbf{a}_1, \dots, \mathbf{a}_K]$ ,  $\mathbf{G} = [\mathbf{g}(f_1), \dots, \mathbf{g}(f_K)]$  denotes the  $N \times K$  temporal response matrix, in which  $\mathbf{g}(f_k) = [g_1(f_k), \dots, g_N(f_k)]^T$ , with  $g_n(f_k) = e^{j2\pi f_k p_n}$  and  $p_n$  being the  $n$ th pulse.  $\mathbf{N}(m) = [\mathbf{n}(p_{m,1}), \mathbf{n}(p_{m,2}), \dots, \mathbf{n}(p_{m,N})]$  is the  $6L \times N$  noise matrix, with  $\mathbf{n}(p_{m,n}) = [\mathbf{n}_1(p_{m,n}), \mathbf{n}_2(p_{m,n}), \dots, \mathbf{n}_L(p_{m,n})]^T$ .  $\mathbf{P}(m) = \text{diag}[\rho_1(p_m), \dots, \rho_K(p_m)]$ .

The objective of this paper is to determine the polarization, angle and frequency parameters  $(\theta_k, \phi_k, \gamma_k, \eta_k, f_k), k = 1, \dots, K$  of the  $K$  targets. We provide a computationally simple solution to the above mentioned problem in Section II, under the following assumptions.

- i) The angle, polarization and frequency parameters  $(\theta_1, \phi_1), \dots, (\theta_K, \phi_K), f_1, \dots, f_K$ , and  $(\gamma_1, \eta_1), \dots, (\gamma_K, \eta_K)$  are pairwise distinct.
- ii) The value  $K$  is known or correctly estimated.
- iii) The target RCS-related coefficients  $\rho_k(t), k = 1, \dots, K$  are of Rayleigh fluctuating, i.e., they are modeled as statistically independent, zero-mean complex Gaussian random processes.
- iv) The noise is zero-mean, complex Gaussian, spatially uniformly white, and is statistically independent of all coefficients  $\rho_k(t), k = 1, \dots, K$ .

## II. POLARIZATION, ANGLE AND FREQUENCY ESTIMATION

### A. Virtual Polarization-Spatial-Temporal Manifold Formulation

We first divide the  $6L \times N$  data block  $\mathbf{X}(m)$  into six  $L \times N$  data blocks, such that each  $L \times N$  data block corresponds to a single EMVA component. Then the  $L \times N$  data block  $\mathbf{X}_i(m)$ , which corresponds to the  $i$ th components of the EMVAs, can be formed out of the  $\mathbf{X}(m)$

$$\mathbf{X}_i(m) = \mathbf{A}\mathcal{D}_i(\mathbf{C})\mathbf{P}(m)\mathbf{G}^T + \mathbf{N}_i(m) \quad (6)$$

where  $\mathcal{D}_i\{\cdot\}$  denotes the operator which takes the  $i$ th row of the matrix in brackets and produces a diagonal matrix by placing this row on the main diagonal. We next concatenate the columns of  $\mathbf{X}_i(m)$  in an  $LN \times 1$  vector  $\mathbf{y}_{i,m}$  as

$$\mathbf{y}_{i,m} = \text{vec}(\mathbf{X}_i(m)) \quad (7)$$

Obviously,  $\mathbf{y}_{i,m}$  has the form

$$\mathbf{y}_{i,m} = (\mathbf{G} \odot \mathbf{A})\mathcal{D}_i(\mathbf{C})\boldsymbol{\rho}(t_m) + \text{vec}(\mathbf{N}_i(m)) \quad (8)$$

where  $\boldsymbol{\rho}(t_m) = [\rho_1(t_m), \dots, \rho_K(t_m)]^T$ ,  $(\mathbf{G} \odot \mathbf{A})$  is the  $LN \times K$  spatial-temporal manifold. For all the  $Q$  data blocks, repeating the operator (7) and arranging the obtained vectors in matrix form, we have

$$\mathbf{Y}_i = [\mathbf{y}_{i,1}, \mathbf{y}_{i,2}, \dots, \mathbf{y}_{i,Q}] = (\mathbf{G} \odot \mathbf{A})\mathcal{D}_i(\mathbf{C})\mathbf{H} + \mathbf{V}_i \quad (9)$$

where  $\mathbf{H} = [\boldsymbol{\rho}(1), \dots, \boldsymbol{\rho}(Q)]$ ,  $\mathbf{V}_i = [\text{vec}(\mathbf{N}_i(1)), \dots, \text{vec}(\mathbf{N}_i(Q))]$ . By using the assumption iii) made in Section ??, the correlation matrix of  $\boldsymbol{\rho}(t_m)$  has the form as

$$\mathbf{R}_\rho = E[\boldsymbol{\rho}(t_m)\boldsymbol{\rho}^H(t_m)] = \text{diag}(\sigma_1^2, \dots, \sigma_K^2) \quad (10)$$

The correlation matrix between data blocks  $\mathbf{Y}_i$  and  $\mathbf{Y}_1$  is then given by

$$\begin{aligned} \mathbf{R}_i &= E[\mathbf{Y}_i\mathbf{Y}_1^H] \\ &= (\mathbf{G} \odot \mathbf{A})\mathcal{D}_i(\mathbf{C})\mathcal{D}_1(\mathbf{C}^*)\mathbf{R}_\rho(\mathbf{G} \odot \mathbf{A})^H + \sigma_n^2\delta_{i,1}\mathbf{I}_{LN} \end{aligned} \quad (11)$$

where  $\sigma_n^2$  is the noise variance, and  $\delta_{i,j}$  denotes the Dirac delta function. Note that the noise terms in (11) are removable by using any existing noise-estimation procedure. For convenience, we regard  $\mathbf{R}_i$  as its noise-free counterparts hereafter. In fact, for the case where noise is taken into account, all the derivations become only approximate.

By vectorizing  $\mathbf{R}_i$ , we can get the following vector

$$\mathbf{r}_i = \text{vec}(\mathbf{R}_i) = [(\mathbf{G} \odot \mathbf{A})^* \odot (\mathbf{G} \odot \mathbf{A})] \mathcal{D}_i(\mathbf{C})\boldsymbol{\beta} \quad (12)$$

where  $\boldsymbol{\beta} = [c_{i,1}^*\sigma_1^2, \dots, c_{i,K}^*\sigma_K^2]^T$ , with  $c_{i,k}$  denoting the  $(i, k)$ th entry of the matrix  $\mathbf{C}$ . Defining the following permutation matrix  $\mathbf{P}$

$$\mathbf{P} = (\mathbf{I}_L \otimes \mathbf{U}_{N^2 \times L})(\mathbf{U}_{N \times L} \otimes \mathbf{I}_{NL}) \quad (13)$$

where  $\mathbf{U}_{P \times Q}$  is a  $PQ \times PQ$  matrix, defined as

$$\mathbf{U}_{P \times Q} = \sum_{i=1}^P \sum_{j=1}^Q \mathbf{E}_{ij} \otimes \mathbf{F}_{ji} \quad (14)$$

where  $\mathbf{E}_{ij}$  is of size  $P \times Q$ , with all zeros except a 1 at the  $(i, j)$ th position, and  $\mathbf{F}_{ji}$  is of size  $Q \times P$ , with all zeros except a 1 at the  $(j, i)$ th position, we can obtain [8]

$$\mathbf{P} [(\mathbf{G} \odot \mathbf{A})^* \odot (\mathbf{G} \odot \mathbf{A})] = [(\mathbf{A}^* \odot \mathbf{A}) \odot (\mathbf{G}^* \odot \mathbf{G})] \quad (15)$$

Then, multiplying the matrix  $\mathbf{P}$  to the vector  $\mathbf{r}_i$ , we can obtain the row-exchanged version of  $\mathbf{r}_i$  as

$$\tilde{\mathbf{r}}_i = \mathbf{P}\mathbf{r}_i = [(\mathbf{A}^* \odot \mathbf{A}) \odot (\mathbf{G}^* \odot \mathbf{G})] \mathcal{D}_i(\mathbf{C})\boldsymbol{\beta} \quad (16)$$

Next, stacking  $\tilde{\mathbf{r}}_i$  for all  $i = 1, \dots, 6$ , we can get  $\tilde{\mathbf{r}} = [\tilde{\mathbf{r}}_1^T, \tilde{\mathbf{r}}_2^T, \dots, \tilde{\mathbf{r}}_6^T]^T$ . It can be easily verified that  $\tilde{\mathbf{r}}$  can be expressed via Khatri-Rao matrix product format as

$$\tilde{\mathbf{r}} = [\mathbf{C} \odot (\mathbf{A}^* \odot \mathbf{A}) \odot (\mathbf{G}^* \odot \mathbf{G})] \boldsymbol{\beta} \quad (17)$$

Obviously, the vector  $\tilde{\mathbf{r}}$  can be considered as a new signal vector with  $6(LN)^2 \times K$  manifold  $\mathbf{C} \odot (\mathbf{A}^* \odot \mathbf{A}) \odot (\mathbf{G}^* \odot \mathbf{G})$  and  $K \times 1$  coefficient  $\boldsymbol{\beta}$ . Moreover,  $\mathbf{C} \odot (\mathbf{A}^* \odot \mathbf{A}) \odot (\mathbf{G}^* \odot \mathbf{G})$  is called as virtual polarization-spatial-temporal (PST) manifold with equivalent polarization manifold  $\mathbf{C}$ , spatial manifold  $(\mathbf{A}^* \odot \mathbf{A})$  and temporal manifold  $(\mathbf{G}^* \odot \mathbf{G})$ .

Using the difference coarray property of the two-level nested array, each column of  $(\mathbf{A}^* \odot \mathbf{A})$  contains  $2L_2(L_1+1)-1$  different elements. These elements can be viewed as spatial response of a  $2L_2(L_1+1)-1$ -element uniform linear array with antennas located from  $(1-L_2(L_1+1))d_1$  to  $(L_2(L_1+1)-1)d_1$ . Similarly, each column of  $(\mathbf{G}^* \odot \mathbf{G})$  contains  $2N_2(N_1+1)-1$  different elements. These elements can be viewed as uniformly sampling of a set of monochromatic signals from time  $(1-N_2(N_1+1))t_1$  to  $(N_2(N_1+1)-1)t_1$ .

By removing the repeated items in  $\mathbf{A}^* \odot \mathbf{A}$  and  $\mathbf{G}^* \odot \mathbf{G}$ , we can form the following vector

$$\bar{\mathbf{r}} = (\mathbf{C} \odot \bar{\mathbf{A}} \odot \bar{\mathbf{G}}) \boldsymbol{\beta} \quad (18)$$

where  $\bar{\mathbf{A}} = [\bar{\mathbf{a}}_1, \dots, \bar{\mathbf{a}}_K]$ , with  $\bar{\mathbf{a}}_k = [e^{-j\frac{2\pi f_c}{c}(1-\bar{L})d_1 \sin \theta_k}, e^{-j\frac{2\pi f_c}{c}(2-\bar{L})d_1 \sin \theta_k}, \dots, e^{-j\frac{2\pi f_c}{c}(\bar{L}-1)d_1 \sin \theta_k}]^T$ , is a  $(2\bar{L}-1 \times K)$  Vandermonde matrix, with  $\bar{L} = L_2(L_1+1)$ , and  $\bar{\mathbf{G}} = [\bar{\mathbf{g}}_1, \dots, \bar{\mathbf{g}}_K]$ , with  $\bar{\mathbf{g}}_k = [e^{j2\pi f_k(1-\bar{N})t_1}, e^{j2\pi f_k(2-\bar{N})t_1}, \dots, e^{j2\pi f_k(\bar{N}-1)t_1}]^T$  is a  $(2\bar{N}-1 \times K)$  Vandermonde matrix, with  $\bar{N} = N_2(N_1+1)$ . In equation (18),  $(\mathbf{C} \odot \bar{\mathbf{A}} \odot \bar{\mathbf{G}})$  behaves like a PST manifold with degrees of freedom  $\mathcal{O}(6(LN)^2)$ . This enhanced degrees of freedom enables to offer better identifiability performance and higher parameter estimation accuracy, as will shown in the subsequent sections.

### B. Direct Data Augmentation for Parameter Identification

In order to exploit the enhanced degrees of freedom for parameter estimation from the vector  $\bar{\mathbf{r}}$ , direct data augmentation technique is adopted. To utilize the direct data augmentation, we divide the manifold matrix  $\bar{\mathbf{A}}$  into  $\bar{L}$  overlapping sub-matrices, where each is of size  $\bar{L} \times K$ . The  $i$ th sub-matrix of  $\bar{\mathbf{A}}$ , which is denoted as  $\bar{\mathbf{A}}_i$ , is composed of the  $(\bar{L}-i+1)$ th to  $(2\bar{L}-i)$ th rows of  $\bar{\mathbf{A}}$ . Analogously, we divide the matrix  $\bar{\mathbf{G}}$  into  $\bar{N}$  overlapping sub-matrices, where each has size  $\bar{N} \times K$ . The  $\ell$ th sub-matrix of  $\bar{\mathbf{G}}$ , which is denoted as  $\bar{\mathbf{G}}_\ell$ , is composed of the  $(\bar{N}-\ell+1)$ th to  $(2\bar{N}-\ell)$ th rows of  $\bar{\mathbf{G}}$ . Then, the vector  $\bar{\mathbf{r}}_{i,\ell}$ , which is associated with  $\bar{\mathbf{A}}_i$  and  $\bar{\mathbf{G}}_\ell$ , can be extracted from  $\bar{\mathbf{r}}$  and expressed as

$$\bar{\mathbf{r}}_{i,\ell} = \mathbf{J}_{i,\ell}\bar{\mathbf{r}} = (\mathbf{C} \odot \bar{\mathbf{A}}_i \odot \bar{\mathbf{G}}_\ell) \boldsymbol{\beta} \quad (19)$$

where  $\mathbf{J}_{i,\ell}$  is the selection matrix, defined as

$$\mathbf{J}_{i,\ell} = \mathbf{I}_6 \otimes \tilde{\mathbf{J}}_i \otimes \bar{\mathbf{J}}_\ell \quad (20)$$

with

$$\tilde{\mathbf{J}}_i = [\mathbf{O}_{\bar{L},\bar{L}-i}, \mathbf{I}_{\bar{L}}, \mathbf{O}_{\bar{L},i-1}] \quad (21)$$

$$\bar{\mathbf{J}}_\ell = [\mathbf{O}_{\bar{N},\bar{N}-\ell}, \mathbf{I}_{\bar{N}}, \mathbf{O}_{\bar{N},\ell-1}] \quad (22)$$

Further, for all  $i = 1, \dots, \bar{L}$  and  $\ell = 1, \dots, \bar{N}$ , we can formulate a  $6\bar{L}\bar{N} \times \bar{L}\bar{N}$  matrix  $\bar{\mathbf{R}}$  as

$$\bar{\mathbf{R}} = [\bar{\mathbf{r}}_{1,1}, \bar{\mathbf{r}}_{1,2}, \dots, \bar{\mathbf{r}}_{1,\bar{N}}, \bar{\mathbf{r}}_{2,1}, \dots, \bar{\mathbf{r}}_{\bar{L},\bar{N}}] \quad (23)$$

We prove in the following theorem that the matrix  $\bar{\mathbf{R}}$  can be applied to subspace-based algorithms for parameter estimation.

*Theorem 1:* The matrix  $\bar{\mathbf{R}}$  defined in (23) can be expressed

$$\bar{\mathbf{R}} = (\mathbf{C} \odot \bar{\mathbf{A}}_1 \odot \bar{\mathbf{G}}_1) \bar{\mathbf{S}} (\bar{\mathbf{A}}_1 \odot \bar{\mathbf{G}}_1)^H \quad (24)$$

where  $\bar{\mathbf{S}} = \text{diag}(\boldsymbol{\beta})$  is a  $K \times K$  diagonal matrix.

*Proof:* The proof is omitted here.

Obviously, the matrix  $\bar{\mathbf{R}}$  has the same structure as the data observed by PST manifold  $(\mathbf{C} \odot \bar{\mathbf{A}}_1 \odot \bar{\mathbf{G}}_1)$  with  $\bar{L}\bar{N}$  samples  $\bar{\mathbf{S}}(\bar{\mathbf{A}}_1 \odot \bar{\mathbf{G}}_1)^H$ . The matrices  $\bar{\mathbf{A}}_1$  and  $\bar{\mathbf{G}}_1$  are both Vandermonde matrices, and hence they are both unambiguous. Therefore, the PST manifold  $(\mathbf{C} \odot \bar{\mathbf{A}}_1 \odot \bar{\mathbf{G}}_1)$  is unambiguous for  $K \leq \bar{L}\bar{N}$ . In order for an polarization-angle-frequency subspace to exist, both  $(\mathbf{C} \odot \bar{\mathbf{A}}_1 \odot \bar{\mathbf{G}}_1)$  and  $(\bar{\mathbf{A}}_1 \odot \bar{\mathbf{G}}_1)$  are required to be tall matrices, i.e.,  $K < \bar{L}\bar{N}$ . Therefore, applying subspace-based algorithms on  $\bar{\mathbf{R}}$  for parameter estimation, up to  $\bar{L}\bar{N}-1$  source signals can be resolved.

### C. Computationally Efficient K-R Signal Subspace Estimation

With the above discussions, subspace-based algorithms can be applied to  $\bar{\mathbf{R}}$  for estimating polarization, angle and frequency parameters. By using the relationship in (24) and performing singular-value decomposition (SVD) to  $\bar{\mathbf{R}}$ , we can find that the  $6\bar{L}\bar{N} \times K$  K-R signal subspace matrix can be obtained by choosing  $K$  left-singular vectors, which are associated with the  $K$  largest singular values of  $\bar{\mathbf{R}}$ . Unfortunately, direct estimation of signal subspace matrix using SVD is computationally intensive, requiring approximately  $(O(\bar{L}\bar{N}))^6$  multiplication operations. To alleviate the computational burden of the SVD, we present a computationally efficient signal subspace estimation method in this subsection.

Let  $\mathbf{D} = (\mathbf{C} \odot \bar{\mathbf{A}}_1 \odot \bar{\mathbf{G}}_1)$  and partition  $\mathbf{D}$  into

$$\mathbf{D} = [\mathbf{D}_1^T, \mathbf{D}_2^T]^T \quad (25)$$

where  $\mathbf{D}_1$  and  $\mathbf{D}_2$  are, respectively the first  $K$  rows and the remaining  $(6\bar{L}\bar{N} - K)$  rows of  $\mathbf{D}$ . As analyzed in Section II-B, for  $K \leq 6\bar{L}\bar{N} - 1$ , the matrix  $\mathbf{D}_1$  is of full rank and is invertible. Therefore, the  $K$  rows of  $\mathbf{D}_1$  are linear independent and the rows of  $\mathbf{D}_2$  can be expressed as linear combinations of these  $K$  rows. Mathematically, there exists a  $K \times (6\bar{L}\bar{N} - K)$  linear operator  $\mathbf{W}$  between  $\mathbf{D}_1$  and  $\mathbf{D}_2$ , such that [12]

$$\mathbf{D}_2 = \mathbf{W}^H \mathbf{D}_1 \quad (26)$$

From (26), we can get

$$\mathbf{D}\mathbf{D}_1^{-1} = \mathbf{E}_s = \begin{bmatrix} \mathbf{I}_K \\ \mathbf{W}^H \end{bmatrix} \quad (27)$$

Since  $\mathbf{D}_1^{-1}$  is nonsingular, it is easily seen that the columns of  $\mathbf{D}$  and  $\mathbf{E}_s$  span the same subspace, i.e., the signal subspace. Therefore, a solution for the signal subspace estimation can be obtained by estimating the linear operator  $\mathbf{W}$ .

In order to estimate the linear operator  $\mathbf{W}$ , we partition the matrix  $\bar{\mathbf{R}}$  into

$$\bar{\mathbf{R}} = [\bar{\mathbf{R}}_1^T, \bar{\mathbf{R}}_2^T]^T \quad (28)$$

where  $\bar{\mathbf{R}}_1$  and  $\bar{\mathbf{R}}_2$  are, respectively the first  $K$  rows and the remaining  $(6\bar{L}\bar{N} - K)$  rows of  $\bar{\mathbf{R}}$ . From (24) and (25),  $\bar{\mathbf{R}}_1$  and  $\bar{\mathbf{R}}_2$  can be expressed as

$$\bar{\mathbf{R}}_1 = \mathbf{D}_1 \bar{\mathbf{S}} (\bar{\mathbf{A}}_1 \odot \bar{\mathbf{G}}_1)^H \quad (29)$$

$$\bar{\mathbf{R}}_2 = \mathbf{D}_2 \bar{\mathbf{S}} (\bar{\mathbf{A}}_1 \odot \bar{\mathbf{G}}_1)^H \quad (30)$$

Therefore, from (26), (29) and (30), the linear operator  $\mathbf{W}$  can be estimated as

$$\mathbf{W} = \mathbf{D}_1^{-H} \mathbf{D}_2^H = (\bar{\mathbf{R}}_1 \bar{\mathbf{R}}_1^H)^{-1} \bar{\mathbf{R}}_1 \bar{\mathbf{R}}_2^H \quad (31)$$

With the estimation of  $\mathbf{W}$ , we can form the estimation of signal subspace matrix  $\mathbf{E}_s$  using (27).

### D. Polarization, Angle and Frequency Estimation

In this subsection, we provide a polarization, angle and frequency estimation method based on the idea of ESPRIT algorithm [15]. Define the following two section matrices

$$\mathbf{J}_{g1} = \mathbf{I}_6 \otimes \mathbf{I}_{\bar{L}} \otimes [\mathbf{I}_{\bar{N}-1}, \mathbf{O}_{\bar{N}-1,1}] \quad (32)$$

$$\mathbf{J}_{g2} = \mathbf{I}_6 \otimes \mathbf{I}_{\bar{L}} \otimes [\mathbf{O}_{\bar{N}-1,1}, \mathbf{I}_{\bar{N}-1}] \quad (33)$$

We can verify that

$$\mathbf{E}_{s1}^\dagger \mathbf{E}_{s2} = \mathbf{D}_1 \Phi_t^* \mathbf{D}_1^{-1} \quad (34)$$

where  $\mathbf{E}_{s1} = \mathbf{J}_{g1} \mathbf{E}_s$  and  $\mathbf{E}_{s2} = \mathbf{J}_{g2} \mathbf{E}_s$ .

Equation (34) establishes the relationship between the linear operator and the phase factors  $\{e^{j2\pi f_k t_1}, k = 1, \dots, K\}$ , which constitute the diagonal elements of  $\Phi_t^*$ . (34) also indicates that the diagonal matrix  $\Phi_t^*$  can be estimated from the eigenvalues of  $\mathbf{E}_{s1}^\dagger \mathbf{E}_{s2}$  and the matrix  $\mathbf{D}_1$  can be estimated from the eigenvectors of  $\mathbf{E}_{s1}^\dagger \mathbf{E}_{s2}$ . With the estimation of  $\Phi_t^*$ , the Doppler frequencies of the targets can be easily calculated as

$$\hat{f}_k = \frac{\arg\{[\Phi_t^*]_{k,k}\}}{2\pi t_1} \quad (35)$$

where  $\arg\{z\}$  signifies the principal argument of the complex number  $z$ .

Using the relationship in (27), the  $6\bar{L}\bar{N} \times K$  PST manifold can be estimated as  $\hat{\mathbf{D}} = \mathbf{E}_s \mathbf{D}_1$ . This  $6\bar{L}\bar{N} \times K$  PST manifold can be divided into six  $\bar{L}\bar{N} \times K$  spatial-temporal (ST) manifolds such that each ST manifold corresponds to a single component of the EMVA. Denoting these six ST manifolds as  $\hat{\mathbf{D}}_{e,1}$ ,  $\hat{\mathbf{D}}_{e,2}$ ,  $\hat{\mathbf{D}}_{e,3}$ ,  $\hat{\mathbf{D}}_{h,1}$ ,  $\hat{\mathbf{D}}_{h,2}$ , and  $\hat{\mathbf{D}}_{h,3}$ , the EMVA manifold  $\mathbf{C}$  can be estimated as

$$\hat{\mathbf{C}} = [\mathcal{M}(\hat{\mathbf{D}}_{e,1})^T, \mathcal{M}(\hat{\mathbf{D}}_{e,2})^T, \mathcal{M}(\hat{\mathbf{D}}_{e,3})^T, \mathcal{M}(\hat{\mathbf{D}}_{h,1})^T, \mathcal{M}(\hat{\mathbf{D}}_{h,2})^T, \mathcal{M}(\hat{\mathbf{D}}_{h,3})^T]^T \quad (36)$$

where  $\mathcal{M}(\cdot)$  denotes the averaging operator that produces a row vector containing the mean value of each column of the matrix in brackets.

Referring back to  $\mathbf{c}_k$  in (4), note that the electric field vector  $\mathbf{e}_k$  and the magnetic field vector  $\mathbf{h}_k$  are orthogonal to each other and to the source signal's Poynting vector  $\mathbf{p}_k$ , whose components are the three direction cosines along the three Cartesian coordinates, i.e.,

$$\mathbf{p}_k = \mathbf{e}_k \times \mathbf{h}_k = \begin{bmatrix} u_k \\ v_k \\ w_k \end{bmatrix} = \begin{bmatrix} \sin \theta_k \cos \theta_k \\ \sin \theta_k \sin \theta_k \\ \cos \theta_k \end{bmatrix} \quad (37)$$

With the estimation of  $\hat{\mathbf{C}}$ , the direction cosine estimates for the  $k$ th target can be obtained by computing the vector cross product between the normalized  $\hat{\mathbf{e}}_k$  and the normalized  $\hat{\mathbf{h}}_k$

$$\begin{bmatrix} \hat{u}_k \\ \hat{v}_k \\ \hat{w}_k \end{bmatrix} = \frac{\hat{\mathbf{e}}_k}{\|\hat{\mathbf{e}}_k\|} \times \frac{\hat{\mathbf{h}}_k}{\|\hat{\mathbf{h}}_k\|} \quad (38)$$

Therefore, the azimuth, elevation and polarization parameters of the  $k$ th target can be estimated as

$$\hat{\theta}_k = \arcsin \left( \sqrt{\hat{u}_k^2 + \hat{v}_k^2} \right) \quad (39)$$

$$\hat{\phi}_k = \angle(\hat{u}_k + j\hat{v}_k) \quad (40)$$

$$\hat{\gamma}_k = \arctan |\hat{d}_{k,1}/\hat{d}_{k,2}| \quad (41)$$

$$\hat{\eta}_k = \angle \hat{d}_{k,1} - \angle \hat{d}_{k,2} \quad (42)$$

where

$$\hat{\mathbf{d}}_k = \begin{bmatrix} d_{k,1} \\ d_{k,2} \end{bmatrix} = \mathbf{Q}^\dagger(\hat{\theta}_k, \hat{\phi}_k) \hat{\mathbf{c}}_k \quad (43)$$

Note that the estimated angle, polarization and frequency parameters are automatically paired without any additional processing.

### III. SIMULATION RESULTS

Simulation results are provided to illustrate the performance of the proposed parameter estimation method. Three competitive methods are considered for comparison. We use the label “Nested-Sampling: Linear Operator” for the proposed method, which uses only linear operator for signal subspace estimation. The method labeled as “Nested-Sampling: Eigendecomposition” uses eigenvalue decomposition for signal subspace estimation. The methods labeled as “Uniformly-Sampling: ESPRIT” and “Uniformly-Sampling: Low Rank Decomposition” use uniformly sampling for data acquisition, and then apply the idea of ESPRIT [13] and low rank decomposition [14] for parameter estimation. For the nested sampling, two stage of nesting in both spatial and temporal domains are considered, with  $L_1 = N_1 = 3$ ,  $L_2 = N_2 = 2$ . For uniformly sampling, a uniformly linear array with 5 antennas and 5 uniformly transmitted pulses are used. Hence, the total number of spatial-temporal data samples is the same for all the four methods. The CPI considered is  $Q = 1000$  for all the methods. The additive noise is assumed to be spatial white complex Gaussian, and the signal-to-noise ratio (SNR) is defined relative to each signal. The result in each of the examples to be considered below is obtained from 500 independent Monte-Carlo trials.

We consider a scenario of two targets with the following parameters to be estimated:  $(f_1, \theta_1, \phi_1, \gamma_1, \eta_1) = (0.1, 10^\circ, 70^\circ, 15^\circ, -90^\circ)$ , and  $(f_2, \theta_2, \phi_2, \gamma_2, \eta_2) = (0.2, 20^\circ, 80^\circ, 45^\circ, 90^\circ)$ . The Doppler frequencies are normalized with respect to the carrier frequency. Fig. 1 shows the root mean squared errors (RMSEs) of the parameter estimates of the first target as a function of SNR varying from 0 dB to 40 dB. From the figure, we see that the nested-sampling based methods have performance better than those of the uniformly-sampling based methods, in terms of lower estimation RMSEs. In addition, we can find that the performance of “Nested-Sampling: Linear Operator” and “Nested-Sampling: Eigendecomposition” are approximately the same, since their RMSE curves nearly overlap.

### IV. CONCLUSIONS

A computationally simple joint angle, polarization and frequency estimation method for pulse doppler radar systems using a linear electromagnetic vector antenna array has been proposed in this paper. Nonuniform spatial-temporal nested sampling is used for data acquisition. RCS diversity is exploited to construct a virtual PST manifold for degrees of freedom enhancement. K-R signal subspace is estimated without performing eigenvalue decomposition. Multiple dimensional target parameters are obtained without pairing computations.

### REFERENCES

- [1] P. Pal and P. P. Vaidyanathan, “Nested array: A novel approach to array processing with enhanced degrees of freedom,” *IEEE Trans. Signal Process.*, vol. 58, no. 8, pp. 4167-4181, Aug. 2010.
- [2] K. Han and A. Nehorai, “Improved source number detection and direction estimation with nested arrays and ULAs using jackknifing,” *IEEE Trans. Signal Process.*, vol. 61, no. 23, pp. 6118-6128, Dec. 2013.
- [3] K. Han and A. Nehorai, “Wideband Gaussian source processing using a linear nested array,” *IEEE Signal Process. Lett.*, vol. 20, no. 11, pp. 1110-1113, Nov. 2013.
- [4] K. Han and A. Nehorai, “Nested array processing for distributed sources,” *IEEE Signal Process. Lett.*, vol. 21, no. 9, pp. 1111-1114, Sept. 2014.
- [5] J. Yang, G. S. Liao, and J. Li, “Robust adaptive beamforming in nested array,” *Signal Process.*, vol. 114, pp. 143-149, 2015.
- [6] Y. Y. Dong, C. X. Dong, Y. T. Zhu, G. Q. Zhao, and S. Y. Liu, “Two-dimensional DOA estimation for L-shaped array with nested subarrays without pair matching,” *IET Signal Process.*, vol. 10, no. 9, pp. 1112-1117, 2016.
- [7] W. Q. Wang and C. L. Zhu, “Nested array receiver with time-delayers for joint target range and angle estimation,” *IET Radar Sonar Navig.*, vol. 10, no. 8, pp. 1384-1393 2016.
- [8] J. He, Z. H. Zhang, T. Shu, B. Tang, and W. X. Yu, “Joint angle-frequency estimation with spatio-temporal nested sampling,” *IET Radar Sonar Navig.*, vol. 11, no. 9, pp. 1373-1378, 2017.
- [9] K. Wang, J. He, T. Shu, and Z. Liu, “Angle-polarization estimation for coherent sources with linear tripole sensor arrays,” *Sensors*, vol. 16, Article 248, 2016.
- [10] A. Nehorai and E. Paldi, “Vector-sensor array processing for electromagnetic source localization,” *IEEE Trans. Signal Process.*, vol. 42, no. 2, pp. 376-398, Feb. 1994.
- [11] J. J. Xiao and A. Nehorai, “Optimal polarized beampattern synthesis using a vector antenna array,” *IEEE Trans. Signal Process.*, vol. 57, no. 2, pp. 576-586, Feb. 2009.
- [12] S. Marcos, A. Marsal, and M. Benidir, “The propagator method for source bearing estimation,” *Signal Process.*, vol. 42, pp. 121-138, 1995.
- [13] A. N. Lemma and A. J. Van der Veen, “Analysis of joint angle-frequency estimation using ESPRIT,” *IEEE Trans. Signal Process.*, vol. 51, no. 5, pp. 1264-1283, May 2003.
- [14] X. Liu and N. D. Sidiropoulos, “Cramér-Rao lower bounds for low-rank decomposition of multidimensional arrays,” *IEEE Trans. Signal Process.*, vol. 49, no. 9, pp. 2074-2086, Sept. 2001.
- [15] R. Roy and T. Kailath, “ESPRIT-estimation of signal parameters via rotational invariance techniques,” *IEEE Trans. Acoust. Speech Signal Process.*, vol. 37, pp. 984-995, July 1989.

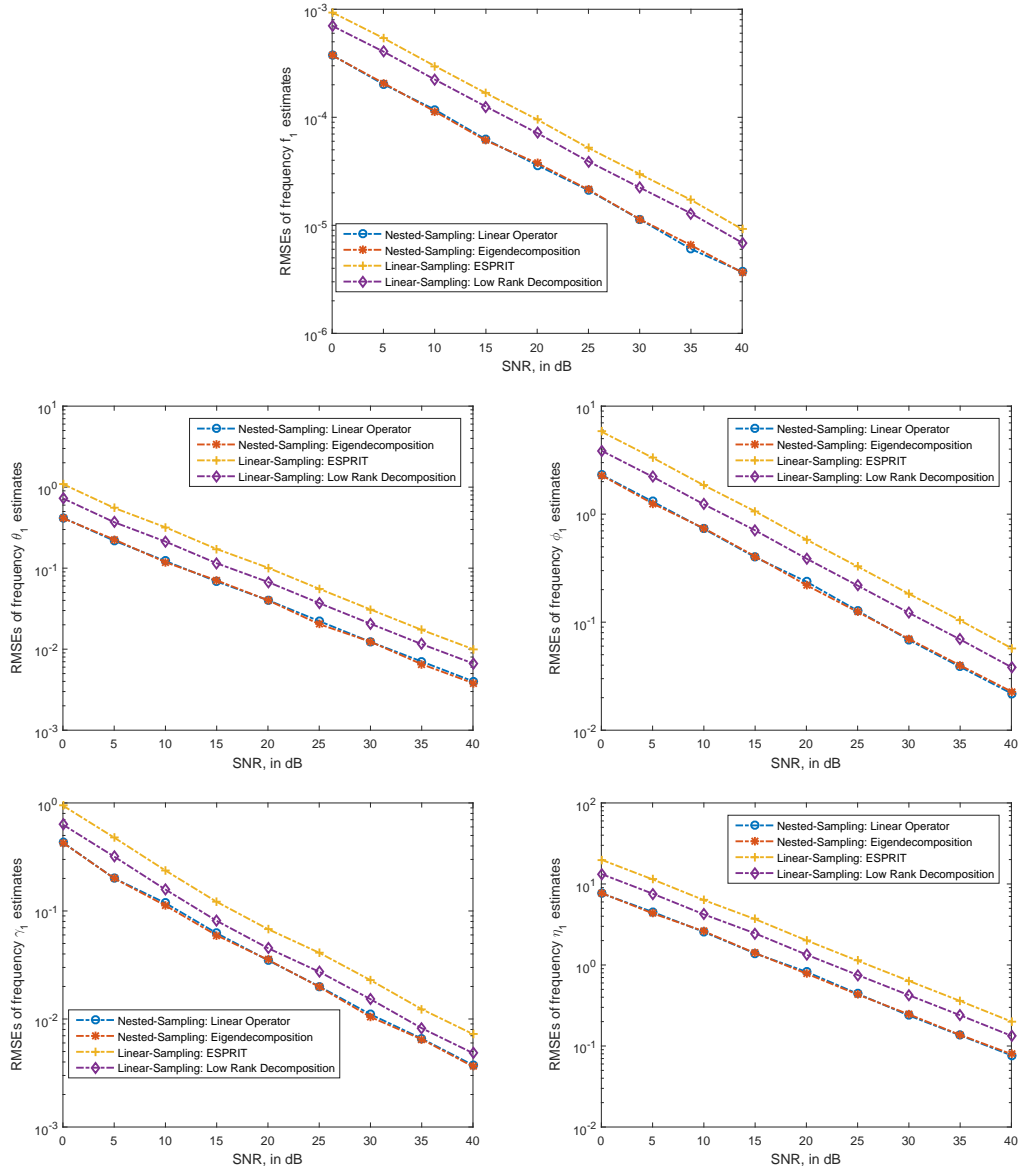


Fig. 1. RMSE of frequency, angle and polarization estimates for the first target versus SNR.  $(f_1, \theta_1, \phi_1, \gamma_1, \eta_1) = (0.1, 10^\circ, 70^\circ, 15^\circ, -90^\circ)$ , and  $(f_2, \theta_2, \phi_2, \gamma_2, \eta_2) = (0.2, 20^\circ, 80^\circ, 45^\circ, 90^\circ)$ .  $Q = 1000$ , 500 independent trials are conducted.